Journal of Cardiovascular Disease Research

ISSN: 0975-3583, 0976-2833 VOL14, ISSUE 09, 2023

Formulation and Characterization of Toremifene Self-Microemulsifying Drug Delivery System for Enhancement of Oral Bioavailability

Ajit Kumar Varma [1], Sarvan[2], Sahil Kumar[3], Rani Kumari[4], Ravi Kumar[5], Rajeev Ranjan[6], Rajat[7], Nihar Ranjan Kar [8], Dr. Mohit Kotnala*

1. Assistant Professor, Faculty of Pharmaceutical Sciences, Rama University, Kanpur(U.P.),India-209217
2. Scholar, HIMT College Of Pharmacy, Plot No. 08 Institutional Area Knowledge Park-I Greater Noida, Pin-201301, Uttar Pradesh
3. Assistant Professor, Aakash Institute of Medical Sciences Nalagarh, Solan - 174101
4. Assistant Professor, Institute of pharmacy, Gopal Narayan Singh University jamuhar Sasaram Bihar -821305
5. Assistant Professor, Faculty of pharmaceutical sciences, Rama university Kanpur Kanpur(U.P.), India-209217
6. Assistant Professor, University Department of Chemistry, DSPM University, Ranchi 834008
7. Assistant Professor, College of Pharmacy, RIMT University, Mandi Gobindgarh Punjab147301
8. Associate Professor, Centurion University of Technology And Management, Gopalpur, Balasore, Odisha, India, Pin-756044

Corresponding: Dr. Mohit Kotnala

Email Id: mohitkotnala198@gmail.com

Affiliation: Science Teacher, Bloom Charter Education, Ain Al Fayedah School-6021 Abu Dhabi United Arab

Abstract: The limited water solubility and dissolution of drugs classified under the Biopharmaceutics Classification System (BCS) class II category provide constraints on their oral bioavailability. In the present study, a self-micro emulsifying drug delivery system (SMEDDS) was employed to enhance the aqueous solubility and oral bioavailability of toremifene, which belongs to the Biopharmaceutics Classification System (BCS) class II category. The selection of Oleic Acid, Transcutol-P, and Span 20 as the oil, surfactant combination, and cosurfactant, respectively, was based on the solubility. The optimal composition (Oleic Acid / Transcutol-P / Span 20 in a volume ratio) for toremifene, which exhibits a small droplet size (132.1 nm) and consistent microemulsification was determined by the use of pseudo-ternary phase diagrams. Differential

ISSN: 0975-3583, 0976-2833 VOL14, ISSUE 09, 2023

scanning calorimetry and powder X-ray diffraction were employed to identify the loss of crystallinity in lyophilized toremifene. The results indicated that toremifene existed in a molecularly dissolved or amorphous state inside the SMEDDS formulation. The saturation solubility and dissolving rate of toremifene -SMEDDS exhibited significant enhancements compared to toremifene powder when tested in water, simulated gastric fluid (pH 1.2), and simulated intestinal fluid (pH 6.8). The female rats exhibited a 1.94-fold increase in the area under the curve and a 1.80-fold increase in the highest plasma concentration following the oral administration of toremifene-SMEDDS compared to the oral administration of the toremifene dispersion. In summary, the findings of our study suggest that self-microemulsifying drug delivery systems (SMEDDS) have promise as an oral formulation for enhancing the therapeutic efficacy of toremifene.

Introduction: Toremifene functions as both an agonist and antagonist of oestrogen in breast and bone tissues, respectively, with the purpose of mitigating the risk of breast cancer and osteoporosis in postmenopausal women.[1] Postmenopausal women experience elevated morbidity and mortality rates due to the presence of osteoporosis and breast cancer. These illnesses exhibit a higher prevalence within this specific community. Hormone replacement therapy is commonly recommended for postmenopausal women as a means to increase oestrogen levels and address associated conditions such as osteoporosis. Nevertheless, the discontinuation of patient treatment is often attributed to the adverse side effects associated with long-term hormone replacement therapy. [2] According to the cited source, it has been suggested that toremifene may be a more favourable choice for postmenopausal women compared to tamoxifen and other selective oestrogen receptor modulators of the first generation. This is attributed to toremifene's enhanced tissue selectivity and reduced incidence of adverse effects.[3] According to clinical practise, the recommended route of administration for toremifene is oral, with a frequency of once daily and a prescribed dosage of 60 mg, aimed at the prevention of postmenopausal osteoporosis. In the human population, toremifene has a comparatively low bioavailability of around 2%, whereas in rats, its bioavailability is estimated to be around 39%. The primary metabolites in rats and humans are Raloxifene 6-D-glucuronide and 4'-D-glucuronide, respectively. These metabolites are formed by phase II glucuronide conjugation in the gut, which serves as a key pathway for tamoxifen metabolism. The presence of many variables necessitated the development of an enhanced oral delivery system to

ISSN: 0975-3583, 0976-2833 VOL14, ISSUE 09, 2023

overcome the limited solubility of tacrolimus.[4] Self-microemulsifying drug delivery systems (SMEDDS) refer to lipid-based formulations that, when encountering the aqueous medium of gastrointestinal secretions and experiencing gentle agitation from peristaltic activity, undergo the formation of tiny oil-in-water (o/w) microemulsions. In order to enhance patient adherence and optimise treatment outcomes, it may be necessary to provide a lower dosage that can still elicit the desired therapeutic effect while minimising gastrointestinal discomfort and other often seen adverse effects. The accelerated drug release patterns and enhanced absorption capabilities are attributed to the inherent characteristics of self-microemulsifying drug delivery systems (SMEDDS), namely their spontaneous change and the reduced particle size. The objective of this investigation was to develop a liquid self-microemulsifying drug delivery system (SMEDDS) containing tacrolimus, which would exhibit enhanced oral bioavailability in comparison to the pure drug powder. [5]

Materials and Methods:

Materials: The oils, including oleic acid, groundnut oil, cotton seed oil, sunflower oil, and soybean oil, were gifts from Gattefossé (Saint-Priest, France), while toremifene was acquired from Tokyo Chemical Industry Co., Ltd. (Tokyo, Japan). N-butanol, Propylene Glycol, and Span 20 were purchased from Sigma-Aldrich (St. Louis, MO, USA), whereas Transcutol-P, Cremophor RH, Labrasol, Span 80, and Tween 20 were screened as surfactants from Daejung Chemical & Metal Co., Ltd. (Siheung, Republic of Korea). All other compounds were either of analytical or high-performance liquid chromatography (HPLC) grade.

Determination of toremifene Solubility in Different Oils, Surfactants, and Co-surfactants: Predetermined amounts of the drug were dissolved in the required quantity of oil. Surfactant and co-surfactant were added to the above mixture as a fixed ratio. Distilled water was added gradually with continuous stirring, which resulted in the formulation of transparent and homogenous self-microemulsifying drug delivery systems (SMEDDS). [6]

HPLC Analysis: The samples obtained from the solubility study were analysed using the Agilent 1200 HPLC system (Agilent Technologies, Santa Clara, CA, USA). The HPLC system was equipped with a G1322A degasser, G1311A quaternary pump, G1314B VWD detector, and an Accucore C18 reversed phase column. The particle size, length, and internal diameter of the column were 2.6 m, 150 mm, and 4.6 mm, respectively. The mobile phase consisted of trimethylamine

ISSN: 0975-3583, 0976-2833 VOL14, ISSUE 09, 2023

(0.2%) and acetonitrile (40:60, v/v), while dilute phosphoric acid was employed to adjust the pH to 4.0. The UV detector wavelength, flow rate, and injection volume were set at 290 nm, 1.0 mL/min, and 20 L, respectively. [7]

In order to establish a calibration curve, a series of toremifene standard solutions were prepared using methanol as the solvent. The calibration curve for toremifene exhibited exceptional linearity, as seen by the R2 value of 0.9999, within the concentration range of 1.5625 to 100 g/mL. The consistency of the calibration curve was demonstrated by several repetitions conducted during the early testing phase. [8]

S. No	Concentration (µg/ml)	Absorbance(nm)
1	2	0.110
2	4	0.201
3	6	0.325
4	8	0.416
5	10	0.512

Table 1: Data for Calibration Curve

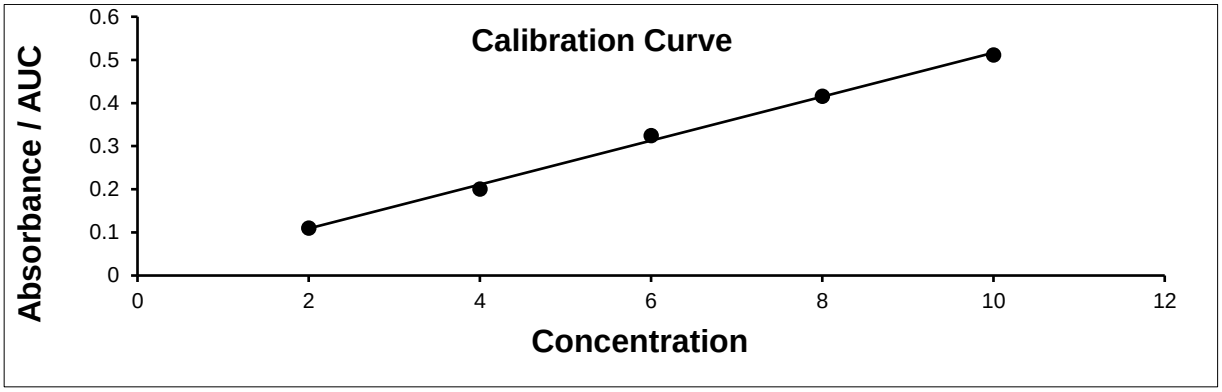

Figure 1: Calibration Curve of toremifene

Construction of Pseudo-Ternary Phase Diagrams: Pseudoternary phase diagrams of oil, surfactant/cosurfactant (Smix), and water were constructed using the aqueous titration method. (10)

ISSN: 0975-3583, 0976-2833 VOL14, ISSUE 09, 2023

The surfactant to cosurfactant mixtures were prepared in ratios of (1:1, 2:1, 3:1, 4:1) then mixed with oil in various weight ratios from 1:9 to 9:1 in multiple glass vials. (11) The resulting homogeneous mixtures of oil/Smix were titrated with water using magnetic stirrer with 50 rpm and at room temperature. After each addition of water, the mixture was checked for phase clarity. The turbidity of different solutions samples would indicate the formation of a coarse emulsion. Where as a clear isotropic solution sample would indicate the formation of a microemulsion. The formation of microemulsion regions was checked visually for turbidity–transparency–turbidity. When the system became turbid, titration was stopped and the percentage of oil, Smix, and water in 100 % w/w mixture were calculated and was utilized for the determination of the microemulsion region boundaries corresponding to the chosen value of oil and Smix ratio. The percentages of oil, surfactants to cosurfactants ratios and water in each system were determined and plotted on triangular coordinated using CHEMIX ternary plot software. [9]

1

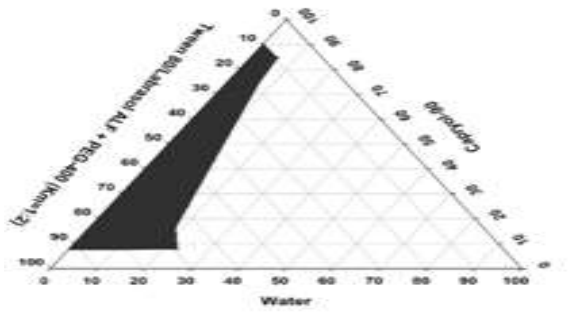

2

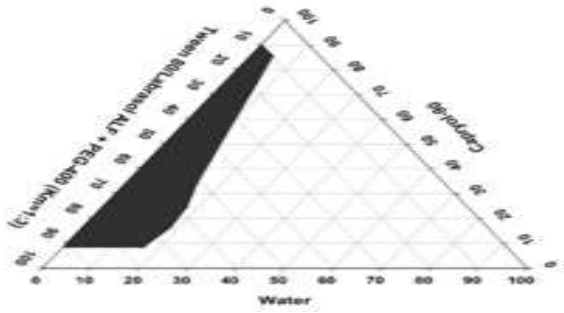

3

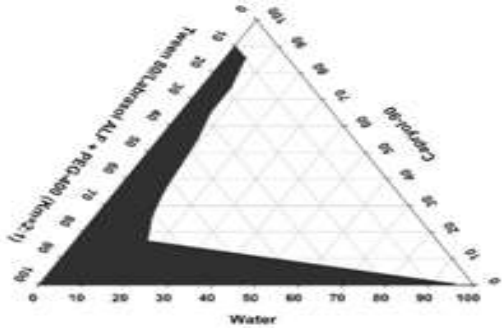

4

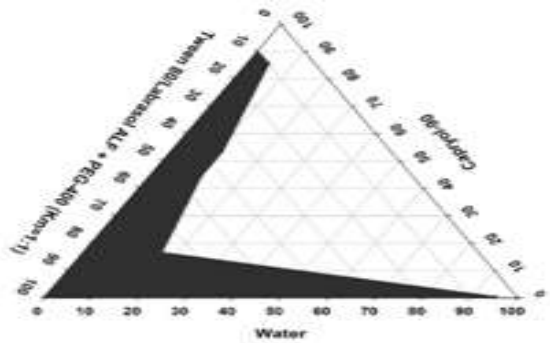

5

ISSN: 0975-3583, 0976-2833 VOL14, ISSUE 09, 2023

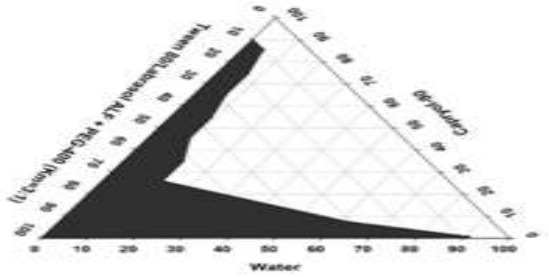

Figure 2: Pseudo-ternary phase diagrams of the self-microemulsifying drug delivery system

Preparation of Liquid and Solid toremifene: Toremifene (0.5mg) was dissolved in Maisine® CC oil with different ratios of selected surfactant and co-surfactant in separate screw-capped glasses vials. They were stirred gently by vortex mixer (50 rpm). The resulting homogenous mixtures were then stored at room temperature. The concentration was 2mg/ml. [10]

Differential scanning calorimetry (DSC) analysis: The process was carried out by weighing two milligram of the pure drug, sealing it in an aluminum pan and then placing in DSC instrument. The sample was heated at temperature up to 300°C and at a rate of 10°C/min, using nitrogen as blank gas. [11]

Droplet Size Analysis and Self-Microemulsifying Behavior of Liquid toremifene SMEDDS: Fine microemulsions were formed by diluting each stable SMEDDS formula with deionized water to 100 times under stirring with a magnetic stirrer at 37°C. Dynamic light scattering method was used to analyze the particle size using particle size analyzer apparatus (Brookhaven, USA) of the resultant micro-emulsions and the PDI was accordingly calculated. [12]

Characterization of Lyophilized Toremifene Self-Microemulsifying Drug delivery system:

Thermodynamic stability studies: Assessing the physical stability of SMEDDS is essential to prevent drug precipitation and excipients phase separation and ensure a good bioavailability and therapeutic drug profile upon administration. (13) Therefore, the prepared formulas were serially assessed by various thermodynamic stability tests with thorough visual observation for any changes in physical appearance. [13]

Centrifugation test: The formulations underwent centrifugation at 3500 rpm for 30 minutes under observation. Stable formulations were then subjected to the freeze-thaw cycle. [14]

ISSN: 0975-3583, 0976-2833 VOL14, ISSUE 09, 2023

Heating-cooling cycle (H/C cycle): Six heating-cooling cycles were performed in which the formulas were placed for 48 hours in alternating temperatures of 4 and 45 °C. The formulas that exhibited no phase separations, creaming or cracking were subjected to centrifugation test. [15]

Freeze-thaw cycle: The formulas were stored for 48 hours at alternating temperatures of -21 and +25 °C for three consecutive cycles. [16]

Formulation	Heating cooling Cycle	Centrifugation	Freeze thaw cycle
OME F1	√	√	√
OME F2	√	√	√
OME F3	×	×	×
OME F4	√	√	√
OME F5	√	√	√
OME F6	×	×	×
OME F7	√	×	×
OME F8	√	√	√
OME F9	√	√	√

√ - Passed ×-Failed

Table 2: Result of Thermodynamic stability assessment of Oleic Acid, Transcutol P, Span 20 containing formulations

Robustness to dilution:

After diluting microemulsion to 50, 100 and 1000 times with water, buffer Ph 7.4 and pH 6.8 and storing for 12 h, it was observed that there was no sign of phase separation or drug precipitation in formulations except OME F3, and OME F6 which turned hazy after standing for long hours. Hence,

ISSN: 0975-3583, 0976-2833 VOL14, ISSUE 09, 2023

formulations OME F3, OME F6, were rejected as they were also showing phase separation and became hazy on dilution. The results were shown in Table. [17]

S.NO	Medium	Phase Separation								
		OME F1	**OME F2**	**OME F3**	**OME F4**	**OME F5**	**OME F6**	**OME F7**	**OME F8**	**OME F9**
1	**Distilled water**	No	No	No	No	No	No	No	No	No
2	**Phosphate buffer pH 6.8Ph**	No	No	Yes	No	No	yes	No	No	No
3	**Phosphate buffer pH7.4**	No	No	Yes	No	No	Yes	No	No	No

Table3: Results of robustness to dilution Oleic Acid, Transcutol P, Span 20 containing formulations

Dispersibility test and self-emulsification time: The efficiency of SMEDDS formulations was assessed using the USP dissolution apparatus II. 1 mL of each formulation was mixed with 500 mL of deionized water at 37 ± 0.5^0C under stirring speed of 50 rpm.(16) The resulting solutions were visually evaluated using the grading system. [18]

Drug content determination: Each formula was dissolved in 100 mL methanol in a volumetric flask and thoroughly mixed. After appropriate filtration and dilution, UV–visible spectrophotometer was used to measure drug absorbance. [19]

Morphological Analysis: Surface morphologies of lyophilized Toremifene-SMEDDS, Toremifene powder, and mannitol were examined using scanning electron microscopy (SEM SU5000; Hitachi, Tokyo, Japan). The powdered samples were fixed on a brass stub with double-sided adhesive tape, coated with platinum under a vacuum using a Hitachi ion sputter, and imaged at an accelerating voltage of 20 kV. [19]

ISSN: 0975-3583, 0976-2833 VOL14, ISSUE 09, 2023

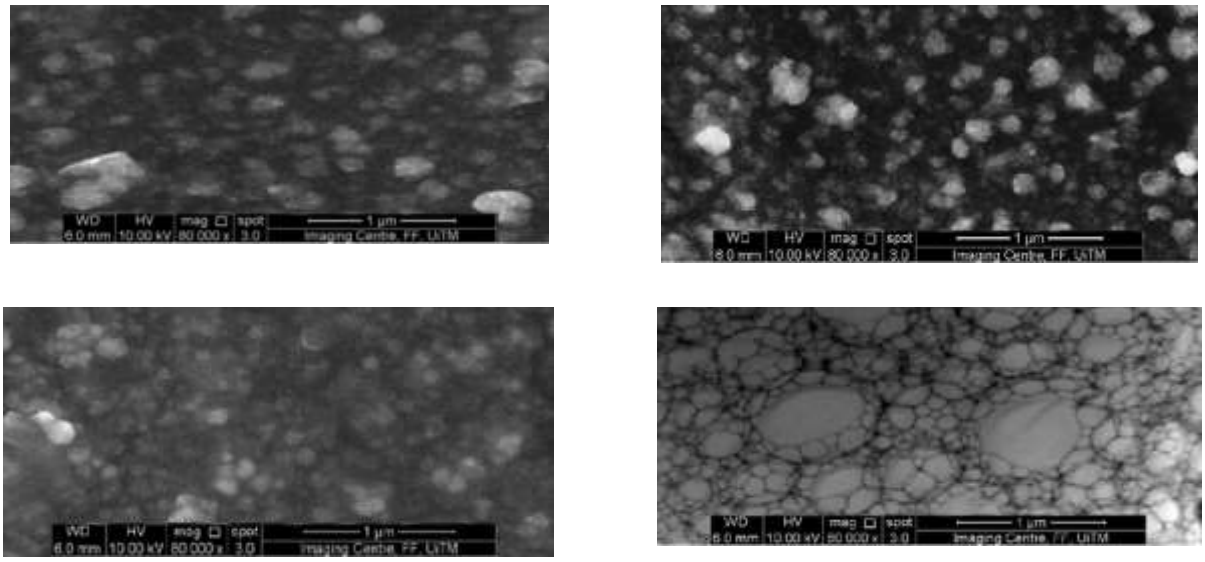

Figure 3. Scanning electron microscopy (SEM) micrographs

Differential Scanning Calorimetry (DSC): A quantity of 2 mg of the drug in its pure form was measured, thereafter enclosed within an aluminium pan, and subsequently introduced into the differential scanning calorimetry (DSC) apparatus in order to carry out the experimental protocol. The sample was subjected to heating using nitrogen as an inert gas, reaching a maximum temperature of 300°C with a heating rate of 10°C per minute. [20]

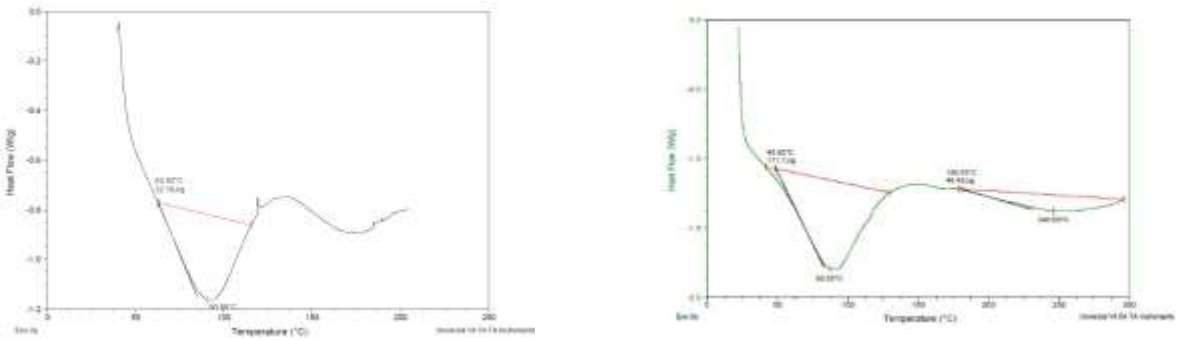

Figure 4: Differential Scanning Calorimetry (DSC)

X-ray Diffraction (PXRD): The powder X-ray diffractometer (D/MAX-2500/PC; Rigaku Corporation, Tokyo, Japan) was used to assess the crystalline states of lyophilized self-microemulsifying drug delivery systems (SMEDDS) and their respective constituent components. The diffractometer utilised a Cu K-α radiation source. The samples underwent scanning within a 2θ

ISSN: 0975-3583, 0976-2833 VOL14, ISSUE 09, 2023

range of 3–70◦, with a step size of 0.02◦. The tube voltage and current were consistently held at 40 kV and 40 mA, respectively. [21]

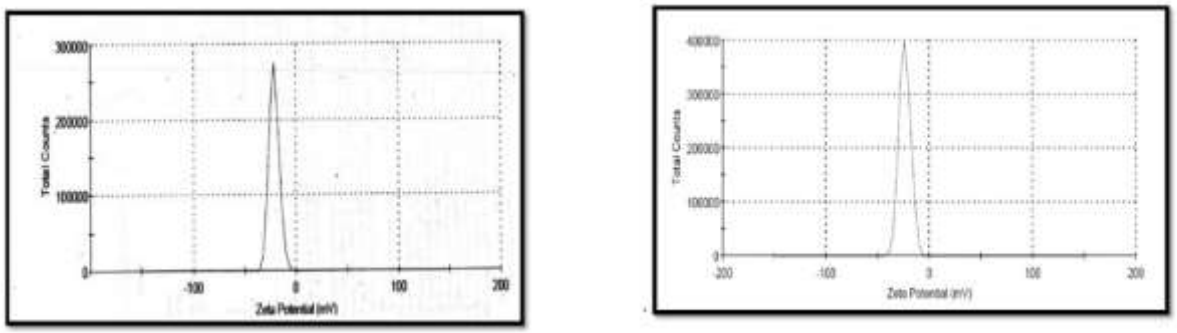

Figure 5: X-ray Diffraction

Fourier-Transform Infrared (FTIR) Spectroscopy: The molecular dynamics of lyophilized Toremifene-SMEDDS were studied using a Fouriertransform infrared spectrophotometer (Alpha II; Bruker, Billerica, MA, USA). The samples were loaded in the disc and spectra were measured over the range of 400–4000 cm^{-1}**.** [22]

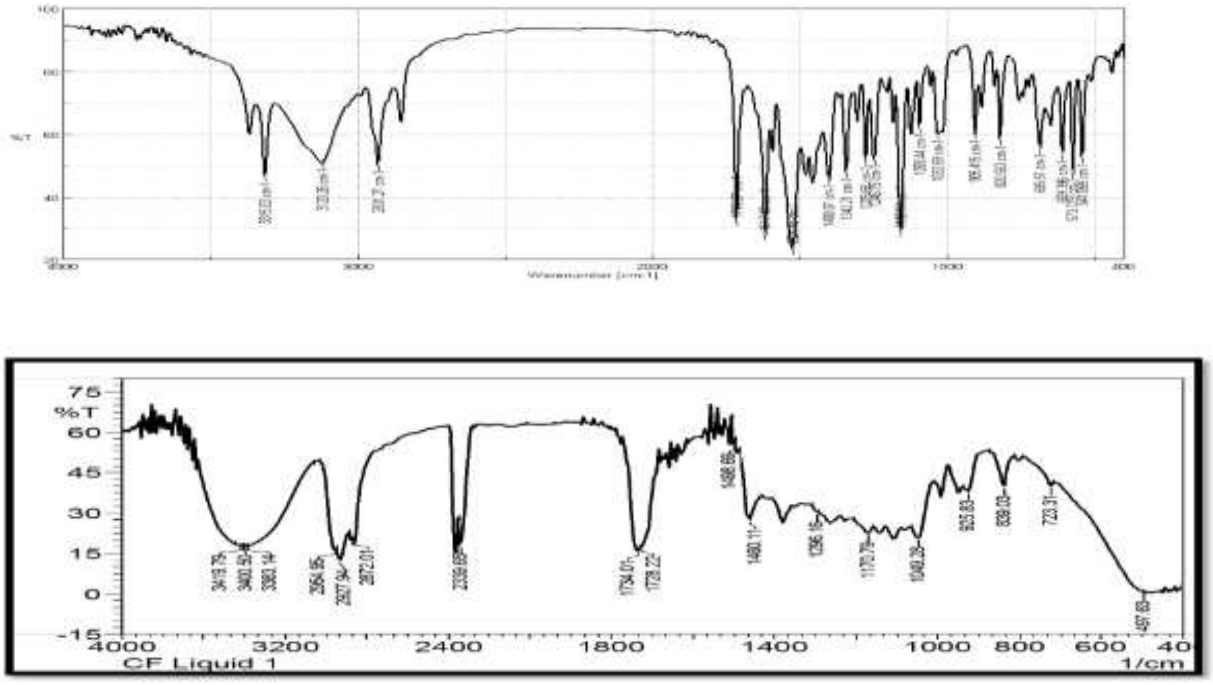

ISSN: 0975-3583, 0976-2833 VOL14, ISSUE 09, 2023

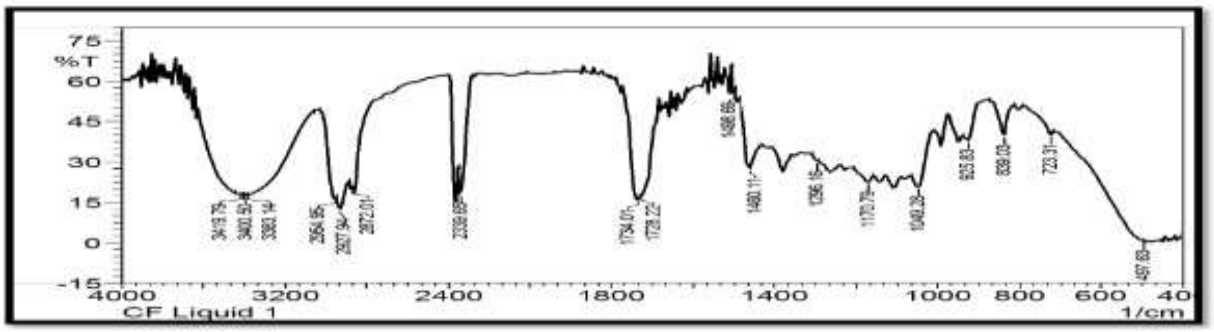

Figure 6: FTIR of drug, surfactant, co-surfactant and oil

Saturation Solubility and In Vitro Dissolution Study of SMEDDS: Using the USP dissolution apparatus-II, the in-vitro release profiles of all prepared formulations along with pure drug were obtained. The dissolution medium consisted of 0.1N HCl at 37±0.5 °C and 75 rpm. (20) Each tacrolimus-loaded SMEDDS formula was placed in a dialysis bag (molecular weight cutoff of 12000 Da), and a regular withdrawal of 5 mL aliquots at 10, 20, 30, 40, 50 and 60 minutes was done. Equal volumes of fresh dissolution media (0.1N HCl) were added to replace the withdrawn samples in order to maintain the volume constant and keep sink condition. The amount of drug dissolved was measured using UV–visible spectrophotometer according to the calibration curve. [23]

In Vivo Pharmacokinetic Study:

Animals: Female Wistar rats (age: 9–10 weeks; weight: 120–20 g) were used to test the in vivo pharmacokinetics of SMEDDS. Before the studies, the animals were provided access to food and water and allowed one week to acclimatise to a typical laboratory environment (25^{o}C average temperature with a 12/12 h light/dark cycle). [24]

Oral Dosing, Blood Sampling, and Plasma Collection: As previously indicated, rats have been used in a pharmacokinetic study. After an overnight period of fasting, a total of four rats were randomly assigned to two groups: Toremifene dispersion and Toremifene SMEDDS. The rats were anaesthetized by an intra-peritoneal injection of zoletil (Vibrac, Westlake, TX, USA) and rompun (Bayer AG, Leverkusen, Germany). Polyethylene tubes manufactured by Clay Adams in Parsippany, NJ, USA were afterwards employed to perform cannulation of the femoral artery for the purpose of blood extraction. The rats were administered either the recently formulated liquid Toremifene-SMEDDS, which was concentrated to a concentration of 5 mg/mL using dimethyl

ISSN: 0975-3583, 0976-2833 VOL14, ISSUE 09, 2023

sulfoxide as a co-solvent, or the Toremifene dispersion, which had a concentration of 5 mg/mL in 0.5% methyl cellulose. The administration was done orally at a dose of 10 mg/kg. Blood samples (120 L) were collected from the femoral artery at certain time intervals: 0, 15, 30, 60, 120, 240, 360, 480, and 1440 minutes. These samples were promptly subjected to centrifugation at 14,000 revolutions per minute (rpm) for a duration of 15 minutes at a temperature of 4 degrees Celsius. The plasma from the supernatant was subsequently separated and stored at a temperature of 20°C until it was ready for analysis. [25]

Sample Preparation, Liquid Chromatography-Tandem Mass Spectrometry (LC-MS/MS) Analysis and Pharmacokinetic Parameters: Utilizing LC MS/MS analysis, the concentration of Toremifene in pharmacokinetic plasma samples was determined. Protein precipitation or deproteinization was used to prepare plasma samples for analysis because it has a variety of benefits, including ease of use, cheap cost, little sample loss, and potential for automation. In order to achieve deproteinization and drug extraction, 50 L of the plasma sample was combined with 100 L of the internal standard solution (100 ng/mL of phenacetin in methanol). The supernatant from the samples was then transferred to an analytical glass vial for LC-MS/MS analysis after centrifuging them at 14,000 rpm for 15 min at 4 C. In a similar manner, a set of calibration standards for rat plasma were made by combining 90 L of blank rat plasma with 10 L of a standard stock solution in methanol to produce final toremifene concentrations of 2, 5, 10, 20, 50, 100, 200, and 500 ng/mL. After that, processing akin to that stated for the plasma samples above was applied, followed by the addition of 200 L of the phenacetin solution as an internal standard (IS). Using an AB SCIEX Triple Quad 3500 (TQ3500) mass spectrometer (AB Sciex LLC, Framingham, MA, U.S.A.) coupled to an Agilent 1290 HPLC system (Agilent Technologies), the generated plasma standards and samples were examined to determine the Toremifene concentration. Utilising a Synergi polar reverse phase column (Phenomenex, Torrance, CA, USA; pore size 80, particle size 4 m, dimensions 150 2 mm) and isocratic elution with acetonitrile and 0.1% aqueous formic acid solution (70:30, v/v) pumped at a flow rate of 0.2 mL/min, chromatographic separation was carried out. [25] The sample injection volume was 2 L, and the autosampler and column were kept at 4 and 25 C, respectively. The positive electrospray ionisation mode of the TQ3500 mass spectrometer was operated via the multiple reaction monitoring (MRM) technique. Maximal sensitivities for Toremifene and IS were attained by optimising MRM and instrument settings. The following were

ISSN: 0975-3583, 0976-2833 VOL14, ISSUE 09, 2023

the toremifene optimal MRM circumstances and MS parameters: Precursor ion mass number is 474.024, product ion mass number is 84.100, declustering potential is 136 V, entrance potential is 10, collision energy is 95 V, collision cell exit potential is 8 V, ion spray voltage is 5500 V, ion source temperature is 500 C, nebulizing gas (GS1) pressure is 25 psi, and drying gas (GS2) pressure is 50 psi. Similar to this, the ideal MS (phenacetin) parameters were as follows: m/z of the precursor ion is 180.035, the product ion is 110.0, the de-clustering potential is 76, the entrance potential is 10, the collision energy is 27 volts, the collision cell exit potential is 8 volts, the ion spray voltage is 5500 volts, the ion source's temperature is 500 degrees Celsius, the nebulizing gas pressure is 50, and the drying gas pressure is also 50 volts. Instrument control, data collection, and analysis were performed using analyst software (version 1.7.2, AB Sciex LLC, Framingham, MA, USA). The Supplementary Material goes into great depth on the LC-MS/MS method's validation. The pharmacokinetic parameters were then determined from the plasma drug concentration data using the WinNonlin® programme and conventional noncompartmental analysis. [26]

Results and Discussion:

Selection of Oil, Surfactants, and Co-surfactants:

Selection of appropriate components is of prime importance for the formation of clear, homogeneous, and stable microemulsions. Solubility is a major parameter in the screening of oils, surfactants, and cosurfactants, as it affects the solubilization capacity of poorly water-soluble drugs in SMEDDS. Toremifene solubility was assessed in different oils, namely Oleic Acid, Groundnut Oil, Cotton seed oil, Sunflower oil, and Soybean oil. Transcutol-P, Cremophor RH, Labrasol, Span 80 and Tween 20 were screened as surfactants, whereas N- butanol, Propylene Glycol and Span 20 were evaluated as cosurfactants. The solubilities of Toremifene in different vehicles are presented in Table 1. Among the various medium- and longchain fatty acid oils, toremifene showed the highest had significantly higher solubility in oleic acid (39.399 mg/ml) as oil phase. Transcutol-P (12.833mg/ml) as surfactant and Span 20 (7.705 mg/ml) as co-surfactants, showed the highest solubility. Therefore, oleic acid, Transcutol-P and Span 20 were selected on the bases of solubility studies for first type of formulation. Medium-chain triglycerides are the preferred choice for lipid-based products because of their high affinity for lipophilic drugs, emulsification properties, and lack of susceptibility to oxidation during long-term storage. Medium-chain triglycerides consisting

ISSN: 0975-3583, 0976-2833 VOL14, ISSUE 09, 2023

of mono- , di-, and triglycerides are commonly used in microemulsions and SMEDDS formulations to enhance the oral absorption of lipophilic drugs. SMEDDS form a stable oil-water emulsion with minimal agitation upon addition to water, as the surfactant and cosurfactant form an interfacial film, reduce the interfacial energy, and improve the thermodynamic stability by preventing coalescence. Nonionic surfactants are generally considered safe and acceptable for oral formulations and have been used in several marketed formulations. Nonionic surfactants pose fewer toxicity concerns than cationic and anionic surfactants, and bulkier surfactants, such as polysorbates, are safer than single-chain surfactants. The Griffin's hydrophilic-lipophilic balance (HLB) scale, designed specifically for nonionic surfactants, ranges between 0 and 20. The HLB system has now been extended to ionic surfactants having much higher HLB values of up to 45, based on their ionization properties. Typically, nonionic surfactants are preferred over ionic surfactants for developing drug formulations as they provide greater resistance to changes in pH or ionic strength. Emulsifiers with HLB values of 3–8 and 8–18 were used to form water-in-oil and oil-in-water microemulsions, respectively. Moreover, stable microemulsions are often formed when a combination of surfactants with different HLB values are used together. [27]

Phase type	**Excipient**	**Solubility (mg/ml)**	**Phase type**	**Excipient**	**Solubility (mg/ml)**	**Phase type**	**Excipient**	**Solubility (mg/ml)**
Oils	Oleic Acid	39.399	**Surfactants**	Transcutol-P	12.833	**Co-Surfactants**	n-butanol	3.31
	Groundnut Oil	26.752		Cremophor RH	9.521			
	Cotton seed oil	27.851		Labrasol	10.271		Propylene Glycol	2.31
	Sunflower oil	28.743		Tween 20	6.532		Span 20	7.705
	Soybean oil	31.220		Span 80	7.34			

ISSN: 0975-3583, 0976-2833 VOL14, ISSUE 09, 2023

Table 4: Solubility study of drug in Oil, Surfactants and Co- Surfactants

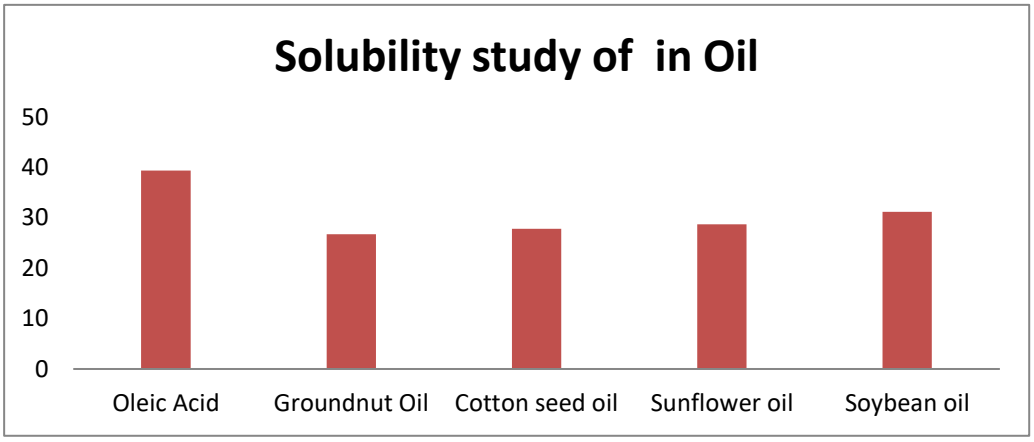

Figure 9: Solubility study of drug in Oleic Acid, Groundnut Oil, Cotton seed oil, Sunflower oil, Soybean oil

Pseudo-Ternary Phase Diagrams:

Pseudo ternary phase diagram was plotted taking different ratio surfactant / co-surfactant ratios as well as changes in the two remaining components (water and oil). For convenience, the phase diagram was constructed by drawing "water dilution lines" representing the increase in oil content and decrease in water level. For both first type of formulation containing oleic acid, Transcutol-P and Span 20 different combinations of oils, water, and surfactant / co-surfactant (S/Cos) were respectively made for research to delineate phase boundaries accurately formed on phase diagrams. Five different systems with surfactant/cosurfactant ratios (Km) of 3:1, 2:1, 1:1, 1:2, and 1:3 were tested. Among the tested compositions, the constructed pseudo-ternary phase diagrams exhibited the largest self-microemulsifying region with a Km ratio of 3:1 (Figure 1A). Upon increasing the proportion of the co-surfactant (2:1, 1:1, 1:2, and 1:3), a gradual decrease in the self-microemulsifying region, and thus, poor emulsion-forming ability, was observed (Figure 1B–E). Areas of self-microemulsifying region were identified as clear and isotropic mixtures. [28]

Optimization of SMEDDS: Various formulations were prepared using different ratios of oil-to-surfactant/cosurfactant combinations, ranging from 1:9 to 1:1. These formulations were developed

ISSN: 0975-3583, 0976-2833 VOL14, ISSUE 09, 2023

based on the selected Km value of 3:1. Table 2 presents the data pertaining to droplet size and microemulsion formation characteristics observed across different ratios of oil and surfactant/cosurfactant mixes, specifically at a constant Km value of 3:1. With the exception of F7 and F8, the findings indicated a significant increase in droplet size when the concentration of surfactant/cosurfactant was decreased in the toremifene -SMEDDS formulations (F1 to F10). At the interface between oil and water, minuscule oil droplets are surrounded by surfactant and cosurfactant molecules, resulting in the formation of the dispersed phase of a microemulsion [55]. The stabilisation and compression of the interfacial coating occur at elevated concentrations of surfactants, resulting in a decrease in particle size [32]. Furthermore, it is possible that the emergence of micelles, as opposed to emulsions, is accountable for the very small size of particles seen at low oil concentrations (F1) [56]. In contrast, the surfactant concentrations in F9 and F10 were found to be low, resulting in inadequate emulsification and an excessively large droplet size. It is important to acknowledge that the initial increments in the ratios of oil to surfactant/co-surfactant combination amounted to 10%. The F3 formulation (20:80) exhibited a particle size exceeding 200 nm together with a very high polydispersity index (PDI), in contrast to the F1 formulation (10:90) which did not yield a microemulsion. Consequently, a novel formulation (referred to as F2) was developed, whereby the oil to surfactant/cosurfactant combination was maintained at a ratio of 15:85. The optimal droplet size and polydispersity index (PDI) were determined in the formulation F2 of toremifene -SMEDDS. This formulation consisted of Capryol 90, Tween 80, Labrasol ALF, and PEG-400 in volume ratios of 150/478.1/159.4/212.5. Figure 2 illustrates a unimodal particle size distribution curve, indicating a homogeneous dispersion of droplets in the toremifene-SMEDDS formulation. Additionally, the low value of polydispersity index (PDI) further supports this observation. Furthermore, it was observed that the improved toremifene -SMEDDS formulation exhibited particle sizes of 119.5 ± 4.6 nm and polydispersity indices (PDIs) of 0.189 ± 0.029 when tested in a physiological buffer with a pH of 1.2. The droplet size and polydispersity index (PDI) of toremifene-SMEDDS in a buffer solution with a pH of 6.8 were measured to be 99.9 ± 4.1 nm and 0.185 ± 0.012, respectively. The particle sizes found in physiological buffers are somewhat smaller in comparison to those in deionized water, which might potentially have a positive impact on gastrointestinal absorption. The impact of droplet size in microemulsions on oral absorption is worth mentioning, since smaller droplets possess a larger surface area, facilitating enhanced absorption. Furthermore, it should be noted that self-microemulsifying drug delivery

ISSN: 0975-3583, 0976-2833 VOL14, ISSUE 09, 2023

systems (SMEDDS) have a characteristic feature of having droplet sizes that are below the threshold of 200 nm, as shown by previous research. The attribute of optical clarity plays a pivotal role in distinguishing microemulsions from conventional emulsions. When SMEDDS are diluted, they exhibit optical clarity, in contrast to emulsions which display optical turbidity. Table 2 displays the transmittance percentages for formulas F1 through F10. Materials that possess optical clarity exhibit a significant degree of light transmission, whereas the opposite is true for materials lacking optical clarity. The formulations ranging from F3 to F5 were subjected to testing in order to assess their optical clarity. The results revealed that these formulations exhibited a transmittance of less than 80%. This finding suggests that these formulations have a tendency to form typical emulsions, while yet maintaining clarity that can be observed without the use of any optical instruments. In contrast, the F2 formulation exhibited high visibility and demonstrated a transmittance value of 96.8%, suggesting that it retained its microemulsion characteristics even after undergoing dilution. The poor transmittance of huge droplets is directly correlated with the percentage of transmittance [34], since they spread the bulk of the incident light. The selection of F2 as a stable optimum formulation was based on the evaluation of many factors including droplet size, polydispersity index (PDI), microemulsifying behaviour, and optical clarity. The existing body of research exhibits considerable ambiguity about the exact characteristics and attributes of SMEDDS and self-nanoemulsifying drug delivery systems (SNEDDS) owing to their significant similarities that often overlap. While there are different droplet size ranges reported in the literature for SMEDDS and SNEDDS, it is worth noting that both formulations exhibit droplet sizes below 250 nm. SNEDDS and SMEDDS are classified as type IIIA and IIIB lipid formulations, respectively, according to the recognised categorization for lipid-based solutions [62,63]. Self-microemulsifying drug delivery systems (SMEDDS) often consist of oil content below 20%, together with higher quantities of hydrophilic surfactants (20-50%) and cosurfactants (20-50%) compared to self-nanoemulsifying drug delivery systems (SNEDDS). SNEDDS, on the other hand, exhibit higher proportions of oil (40-80%).[28] In addition, as compared to microemulsions, nanoemulsions exhibit thermodynamic instability. Nanoemulsions often need the use of external energy, such as high-pressure homogenization or ultrasonication, to convert separate components into a colloidal dispersion. In contrast, microemulsions may be formed with mild agitation of oil, water, and surfactants [64]. During the course of our analysis, it was observed that the Toremifene-SMEDDS formulation exhibited an oil content of less than 20%. This formulation was created

ISSN: 0975-3583, 0976-2833 VOL14, ISSUE 09, 2023

utilising a simple method including mild heating and stirring. The identification of self-microemulsifying zones was accomplished by the utilisation of a water titration method, which facilitated the creation of pseudo ternary phase diagrams. The formation of a microemulsion, as opposed to a nanoemulsion, in our study can be attributed to several factors. Firstly, the particle size falls within the specified range. Additionally, the composition of the formulation is comparable to type III B lipid formulation. Moreover, the preparation method does not involve the use of external energy. Furthermore, the emulsification behaviour exhibited by the formulation is noteworthy. Lastly, the stability of the formulation, as evidenced by the absence of any phase separation throughout the study, further supports the conclusion that a microemulsion was indeed formed. The utilisation of SMEDDS, as opposed to SNEDDS, more accurately encapsulates the fundamental nature of our notion. [29]

Formulation code	Conductivity	(%) Drug Content	Polydispersity index (PDI)	Entrapment efficiency (%)	Particle size (nm)
OME F1	0.183	91.06	0.839	82.2±2.1	51.0±7.1
OME F2	0.192	90.56	0.447	80.1±2.2	47.0±1.1
OME F3	0.189	98.11	0.368	85.4±2.7	51.0±8.1
OME F4	0.199	99.23	0.268	89.6±4.6	41.3±5.7
OME F5	0.201	96.10	0.272	89.3±5.6	41.0±7.1
OME F6	0.176	95.97	0.478	65.5±2.4	48.9±7.8
OME F7	0.180	93.38	0.612	73.6±0.8	62.5±5.5
OME F8	0.179	93.71	0.475	85.3±0.8	46.0±4.2
OME F9	0.191	90.37	0.536	78.7±1.8	81.4±6.2

Table 5: Evaluation parameters

Solid State Characteristics of SMEDDS: The thermal behaviours of toremifene powder, mannitol, the physical combination, and lyophilized toremifene SMEDDS are depicted in the DSC

ISSN: 0975-3583, 0976-2833 VOL14, ISSUE 09, 2023

thermograms presented in Figure 4A. Both mannitol and toremifene powder exhibited significant endothermic peaks at temperatures about 268 and 168°C, respectively, aligning with their respective melting points. The endothermic peaks seen in the physical mixture (1:1) of toremifene and mannitol exhibited different characteristics. Specifically, the endothermic peak for toremifene at 230.5°C was less prominent and more rounded, whereas the endothermic peak for mannitol at 168.3 °C appeared sharper. The decrease in crystallinity and the appearance of a lower intensity peak at a somewhat lower temperature in the melting endotherm of toremifene in the physical combination might perhaps be attributed to the partial dissolution of toremifene in molten mannitol [65]. In contrast, the endothermic peak observed in the differential scanning calorimetry thermogram of lyophilized toremifene SMEDDS entirely disappeared, indicating the full dissolution of the chemical inside the formulation and its transformation from an initial crystalline form to an amorphous state. The thermogram of toremifene SMEDDS continues to exhibit the endothermic melting peak for mannitol, but at a slightly reduced temperature of 163.6°C. [30]

Dissolution Profile of SMEDDS: saturation solubilities of toremifene powder and lyophilized toremifene- SMEDDS in different physiological media are presented in figure 6. moreover, the ph-solubility profile of toremifene is shown in the supplementary material figure s1. at equilibrium, the saturation solubility of toremifene-SMEDDS in water (225.3 vs. 15.2 µg/mL), sgf (142.2 vs. 16.0 µg/ml), and sif (178.9 vs. 1.7 µg/ml) was substantially higher than that of toremifene powder (figure 6). these results indicate that toremifene-smedds significantly improved the saturation solubility of toremifene by 14.8-, 8.9-, and 105-fold increases in water, sgf, and sif, respectively. the increased saturation solubility of toremifene-smedds can be ascribed to the smaller particle size and amorphous nature of toremifene within the smedds formulation. these factors collectively enhance the partitioning of the drug into lipid droplets and potential micelles, leading to improved saturation solubility. In vitro dissolution profiles of lyophilized toremifene SMEDDS and toremifene powder in different dissolution media are shown in figure 7. toremifene powder had a noticeably low dissolution rate owing to its poor solubility in media. approximately 30–60% of the toremifene powder was dissolved in 110 min, and the cumulative drug dissolution was in the order of sgf (60.8%) > water (46.9%) > sif (30.2%). the dissolution profiles of toremifene powder were consistent with the saturation solubility results, and the higher dissolution rate of toremifene in SGF could be ascribed to its higher solubility than that in sif. in contrast, the toremifene-SMEDDS

ISSN: 0975-3583, 0976-2833 VOL14, ISSUE 09, 2023

showed substantially higher dissolution rates than toremifene powder in each dissolution medium. from figure 7, it is evident that approximately 80% of toremifene was dissolved from toremifene SMEDDS in the first 60 min in all 3 media. these enhanced toremifene disso- lution velocities could be ascribed to the fact that completely dissolved toremifene in SMEDDS was quickly released into the medium by the spontaneous formation of small droplets. the collective contributions from the molecularly dissolved/amorphous state of the drug, improved saturation solubility, small droplet size, and low interfacial energy resulted in the higher dissolution rate of toremifene SMEDDS compared to that of toremifene powder. [31]

Pharmacokinetics Profile: A simple, reliable, and sensitive LC-MS/MS method was developed to determine toremifene concentrations in rat plasma samples. The optimized MRM and chromatographic conditions resulted in efficient peak resolution, with sharp peaks for toremifene and phenacetin at 3.37 and 2.35 min, respectively. These retention times for toremifene and the IS remained almost the same for all standard and plasma samples which demonstrate adequate selectivity of the method. The calibration curve for toremifene in rat plasma constructed in the concentration range of 2–500 ng/mL showed very good linearity, as demonstrated by a high coefficient of correlation ($r = 0.9992$ with a weighing factor of 1/x). The accuracy for all the standard concentrations was between 89.9% and 110%. These results indicate that response (toremifene to IS peak area ratio) is directly proportional to the toremifene to IS concentration ratio in plasma samples, thus showing linearity of the method. [32]

The intraday accuracy and precision at four different QC concentrations of toremifene in rat plasma is shown in the Supplementary Material Table S1. The intraday accuracy for toremifene was in the range of 95.17–107.58% with absolute %RE of 0.39–7.58%. Similarly, the intraday precision for toremifene in QC samples was found to be 3.171%. The accuracy and precision data for toremifene was well within the acceptable limits of 20% for LLOQ and 15% for all other QC samples, as specified by the US-FDA guidelines for bioanalytical methods validation. The recovery, extraction efficiency, and matrix effects were also evaluated at four different QC concentrations of toremifene using five different sources of rat plasma and the results are shown in the Supplementary Material Table S2. As shown in the results, total recovery and extraction efficiency ranged between 90.75% and 99.25% and 94.76% and 96.35%, respectively, for all QC samples. These finding suggests the suitability of the protein precipitation method to adequately extract toremifene from rat plasma.

ISSN: 0975-3583, 0976-2833 VOL14, ISSUE 09, 2023

Furthermore, the absolute matrix effect was also similar for all QC levels (94.28–103.09%) in all plasma sources. The relative matrix effect, which shows the variability in peak areas of toremifene spiked in extracted plasma samples in the same concentration level, was also comparable between different QC levels. The relative matrix effect ranged between 1.09% and 3.07% for all QC levels, which indicates the absence of a significant effect from the plasma matrix for the analysis of toremifene in rat plasma. Taken together, the results of method validation demonstrated the adequacy and suitability of the developed LC-MS/MS method. [32]

The in vivo pharmacokinetics study for toremifene SMEDDS was conducted in female rats at a dose of 10 mg/kg. This dose for rats was decided by converting the daily recommended dose of toremifene in human (60 mg daily, or 1 mg/kg assuming average human body weight of 60 kg) to animal equivalent dose. According to the US-FDA guidance, the intercon- version of human and animal equivalent doses are based on the concept of conversion factor calculated by normalization of dose to body surface area. By using human to animal dose conversion, rat equivalent dose was calculated as 6.2 mg/kg. Based on these calculations and a pilot pharmacokinetics study, we used a slightly higher dose of 10 mg/kg for pharmacokinetics study in rats. Plasma drug concentration vs. time profiles of toremifene SMEDDS and toremifene dispersion after oral administration to female rats are shown in Figure 8. toremifene SMEDDS exhibited a higher plasma drug concentration than toremifene dispersion, and the difference in plasma concentration was more prominent after 120 min. The noncom- partmental pharmacokinetics parameters calculated from the plasma toremifene concentration vs. time data. Toremifene SMEDDS exhibited significantly higher area under the concentration-time curve from 0 to 24 h (AUC_{24h}; 87,144.5 vs. 44,907.5 ng min/mL; $p < 0.01$) and maximum concentration (C_{max}; 81.6 vs. 45.6 ng/mL; $p < 0.05$) than toremifene dispersion. Both AUC_{24h} and C_{max} are key indicators for describing and comparing the oral bioavailability of formulations. Furthermore, the relative bioavailability (BA_{rel}) of toremifene SMEDDS was 194% of that of the toremifene dispersion. The enhanced absorption and oral bioavailability of toremifene SMEDDS may be attributed to the large surface area provided by tiny microemulsion droplets and improved diffusion, solubility, and dissolution in the gastrointestinal tract, and enhanced mucosal permeability due to surfactants. Indeed, toremifene dispersion exhibited poor and slow absorption owing to its very low solubility and slow dissolution rate in intestinal fluid, as evidenced by its saturation solubility and dissolution profile. Although toremifene SMEDDS improved the oral

ISSN: 0975-3583, 0976-2833 VOL14, ISSUE 09, 2023

bioavail- ability of toremifene by almost two-fold, the time to reach the maximum drug concentration (T_{max}) was long, and the overall plasma drug concentration was lower than that expected from the solubility and dissolution data. The slightly delayed absorption and long T_{max} of toremifene SMEDDS may be due to a very long elimination half-life of toremifene and the possible contribution and involvement of the intestinal lymphatic pathway. [33]

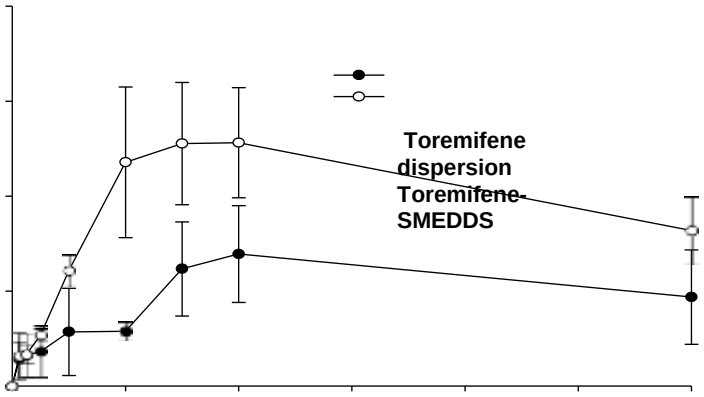

Figure 10: Average toremifene plasma concentration–time profiles after the oral administration of toremifene dispersion and toremifene -SMEDDS to female rats at a dose equivalent to 10 mg/kg. Data are represented as the mean ± S.D. (n = 4).

Toremifene possesses an elimination half-life of 27–32 h in humans because of reversible systemic metabolism and significant enterohepatic cycling of the drug. Since T_{max} is governed by the rates of drug absorption and elimination, slow absorption and elimination of drugs result in high T_{max} values. Slow lymphatic flow may also contribute to slow absorption and delayed T_{max} of toremifene SMEDDS; such findings with lymphatic absorption have also been previously reported. In addition, presystemic glucuronide metabolism of toremifene in the intestine is a major determining step for oral absorption that may affect the pharmacokinetic parameters of toremifene SMEDDS. Finally, low water content (3.2 mL) in the gastrointestinal tract of fasted rats may also affect the self-microemulsifying process of SMEDDS, and thus, the oral absorption. [34] Previously, somewhat comparable pharmacokinetic results have been reported for toremifene in studies intended to improve its oral bioavailability via nanostructured lipid carriers (NLCs). NLCs prepared from glyceryl tribehenate and oleic acid resulted in a 3.19-fold enhancement in oral bioavailability compared to toremifene suspension at a dose of 15 mg/kg. In another study, NLCs formulated with

ISSN: 0975-3583, 0976-2833 VOL14, ISSUE 09, 2023

glyceryl monostearate and Capmul MCM C8 showed a 3.75-fold increase in oral bioavailability compared to toremifene. [34]

Conclusions: In this study, we successfully developed an SMEDDS formulation for the effective oral delivery of the poorly water-soluble drug, toremifene. The formulation components and their pro- portional ratios were determined through a solubility study, construction of pseudo-ternary phase diagrams, droplet size, and emulsification ability measurements. The developed toremifene SMEDDS successfully enhanced the solubility and dissolution of toremifene in different physiological media, namely water, SGF, and SIF. Furthermore, key pharmacokinetic parameters of toremifene, such as AUC and C_{max}, were also significantly improved by toremifene SMEDDS after oral administration to rats, indicating improved in vivo absorption compared to that of toremifene powder. Therefore, SMEDDS is a promising formulation that can overcome the drawbacks associated with the poor solubility and oral bioavailability of toremifene.

REFERENCES

1. Agnihotri, S., Mukherji, S., and Mukherji, S. (2013). Immobilized Silver Nanoparticles Enhance Contact Killing and Show Highest Efficacy: Elucidation of the Mechanism of Bactericidal Action of Silver. *Nanoscale* 5 (16), 7328–7340. doi:10.1039/c3nr00024a
2. Ajitha, B., Ashok Kumar Reddy, Y., and Sreedhara Reddy, P. (2015). Green Synthesis and Characterization of Silver Nanoparticles Using Lantana Camara Leaf Extract. *Mater. Sci. Eng. C* 49, 373–381. doi:10.1016/ j.msec.2015.01.035
3. Akintelu, S. A., Bo, Y., and Folorunso, A. S. (2020). A Review on Synthesis, Optimization, Mechanism, Characterization, and Antibacterial Application of Silver Nanoparticles Synthesized from Plants. *J. Chem.* 2020, 3189043. doi:10.1155/2020/3189043
4. Albrecht, M. A., Evans, C. W., and Raston, C. L. (2006). Green Chemistry and the Health Implications of Nanoparticles. *Green. Chem.* 8 (5), 417–432. doi:10.1039/b517131h
5. Anandalakshmi, K., Venugobal, J., and Ramasamy, V. (2016). Characterization of Silver Nanoparticles by green Synthesis Method Using Pedalium Murex Leaf Extract and Their Antibacterial Activity. *Appl. Nanosci.* 6 (3), 399–408. doi:10.1007/s13204-015-0449-z

ISSN: 0975-3583, 0976-2833 VOL14, ISSUE 09, 2023

6. Bin Sayeed, M., Karim, S., Sharmin, T., and Morshed, M. (2016). Critical Analysis on Characterization, Systemic Effect, and Therapeutic Potential of Beta- Sitosterol: a Plant-Derived Orphan Phytosterol. *Medicines* 3 (4), 29. doi:10.3390/medicines3040029
7. Bondarenko, O., Juganson, K., Ivask, A., Kasemets, K., Mortimer, M., and Kahru, (2013). Toxicity of Ag, CuO and ZnO Nanoparticles to Selected Environmentally Relevant Test Organisms and Mammalian Cells *In Vitro*: a Critical Review. *Arch. Toxicol.* 87 (7), 1181–1200. doi:10.1007/s00204-013- 1079-4
8. Botten, D., Fugallo, G., Fraternali, F., and Molteni, C. (2015). Structural Properties of Green Tea Catechins. *J. Phys. Chem. B* 119 (40), 12860–12867. doi:10.1021/ acs.jpcb.5b08737
9. Carbin, B.-E., Larsson, B., and Lindahl, O. (1990). Treatment of Benign Prostatic Hyperplasia with Phytosterols. *Br. J. Urol.* 66 (6), 639–641. doi:10.1111/j.1464-410x.1990.tb07199.x
10. Castillo-Henríquez, L., Alfaro-Aguilar, K., Ugalde-Álvarez, J., Vega-Fernández, L., Montes de Oca-Vásquez, G., and Vega-Baudrit, J. R. (2020). Green Synthesis of Gold and Silver Nanoparticles from Plant Extracts and Their Possible Applications as Antimicrobial Agents in the Agricultural Area. *Nanomaterials* 10 (9), 1763. doi:10.3390/nano10091763
11. Castro, L., Blázquez, M. L., Muñoz, J. á., González, F. G., and Ballester, A. (2014). Mechanism and Applications of Metal Nanoparticles Prepared by Bio- Mediated Process. *Rev. Adv. Sci. Engng* 3 (3), 199–216. doi:10.1166/ rase.2014.1064
12. CDC (2013). *Antibiotic Resistance Threats in the United States*. U. S. Department of Health and Human Services, Centers for Disease Control and Prevention.
13. Chattopadhyay, S., Dash, S. K., and Ghosh, T. (2010). Surface modification of cobalt oxide nanoparticles using phosphonomethyl iminodiacetic acid followed by folic acid: a biocompatible vehicle for targeted anticancer drug delivery. *Cancer Nano.* 4, 103–116. doi:10.1007/s12645-013-0042-7
14. Das, R., Nath, S. S., Chakdar, D., Gope, G., and Bhattacharjee, R. (2010). Synthesis of Silver Nanoparticles and Their Optical Properties. *J. Exp. Nanoscience* 5 (4), 357–362. doi:10.1080/17458080903583915

ISSN: 0975-3583, 0976-2833 VOL14, ISSUE 09, 2023

15. Dickson, J. S., and Koohmaraie, M. (1989). Cell Surface Charge Characteristics and Their Relationship to Bacterial Attachment to Meat Surfaces. *Appl. Environ. Microbiol.* 55 (4), 832–836. doi:10.1128/aem.55.4.832-836.1989
16. Durán, N., Nakazato, G., and Seabra, A. (2016). Antimicrobial Activity of Biogenic Silver Nanoparticles, and Silver Chloride Nanoparticles: an Overview and Comments. *J Appl. Microbiol. Biotechnol.* 100 (15), 6555–6570. doi:10.1007/ s00253-016-7657-7
17. ECDC (2018). "European Centre for Disease Prevention and Control; Antimicrobial Resistance Surveillance in Europe 2017," in *Annual Report of the European Antimicrobial Resistance Surveillance Network (EARS-Net)* (Stockholm: ECDC). doi:10.2900/797061
18. Eram, R., Kumari, P., Panda, P. K., Singh, S., Sarkar, B., Mallick, M. A., et al. (2021). Cellular Investigations on Mechanistic Biocompatibility of Green Synthesized Calcium Oxide Nanoparticles with *Danio rerio*. *J. Nanotheronastics.* 2 (1), 51–62. doi:10.3390/jnt2010004
19. Forester, S. C., and Lambert, J. D. (2011). The Role of Antioxidant versus Pro- oxidant Effects of green tea Polyphenols in Cancer Prevention. *Mol. Nutr. Food Res.* 55 (6), 844–854. doi:10.1002/mnfr.201000641
20. Fox, C. L., and Modak, S. M. (1974). Mechanism of Silver Sulfadiazine Action on Burn Wound Infections. *Antimicrob. Agents Chemother.* 5 (6), 582–588. doi:10.1128/aac.5.6.582
21. Ghante, M. H., and Jamkhande, P. G. (2019). Role of Pentacyclic Triterpenoids in Chemoprevention and Anticancer Treatment: An Overview on Targets and Underling Mechanisms. *J. Pharmacopuncture* 22 (2), 55–67. doi:10.3831/ KPI.201.22.007
22. Gholami, M., Shahzamani, K., Marzban, A., and Lashgarian, H. E. (2018). Evaluation of Antimicrobial Activity of Synthesised Silver Nanoparticles Using Thymus Kotschyanus Aqueous Extract. *IET nanobiotechnol.* 12 (8), 1114–1117. doi:10.1049/iet-nbt.2018.5110
23. Gong, P., Li, H., He, X., Wang, K., Hu, J., Tan, W., et al. (2007). Preparation and Antibacterial Activity of Fe3O4@Ag Nanoparticles. *Nanotechnology* 18 (28), 285604. doi:10.1088/0957-4484/18/28/285604
24. Guzmán, M. G., Dille, J., and Godet, S. (2009). Synthesis of Silver Nanoparticles by Chemical Reduction Method and Their Antibacterial Activity. *Int. J. Chem. Biomol. Eng.* 2 (3), 104–111.

ISSN: 0975-3583, 0976-2833 VOL14, ISSUE 09, 2023

25. Hajiaghaalipour, F., Sanusi, J., and Kanthimathi, M. S. (2016). Temperature and Time of Steeping Affect the Antioxidant Properties of white, green, and Black tea Infusions. *J. Food Sci.* 81 (1), H246–H254. doi:10.1111/1750- 3841.13149
26. Hamouda, R. A., Hussein, M. H., Abo-emlagd, R. A., and Bawazir, S. S. (2019). Synthesis and Biological Characterization of Silver Nanoparticles Derived from the Cyanobacterium Oscillatoria Limnetica. *Sci. Rep.* 9 (1), 13071. doi:10.1038/ s41598-019-49444-y
27. Husain, S., Verma, S. K., Hemlata, fnm., Azam, M., Sardar, M., Haq, Q. M. R., et al. (2021). Antibacterial Efficacy of Facile Cyanobacterial Silver Nanoparticles Inferred by Antioxidant Mechanism. *Mater. Sci. Eng. C* 122, 111888. doi:10.1016/j.msec.2021.111888
28. Husain, S., Verma, S. K., Yasin, D., Hemlata, F., A. Rizvi, M. M., and Fatma, T. (2021). Facile green Bio-Fabricated Silver Nanoparticles from Microchaete Infer Dose-dependent Antioxidant and Anti-proliferative Activity to Mediate Cellular Apoptosis. *Bioorg. Chem.* 107, 104535. doi:10.1016/ j.bioorg.2020.104535
29. Jafari, A., Jafari Nodooshan, S., Safarkar, R., Movahedzadeh, F., Mosavari, N., Novin Kashani, A., et al. (2018). Toxicity Effects of AgZnO Nanoparticles and Rifampicin on *Mycobacterium tuberculosis* into the Macrophage. *J. Basic Microbiol.* 58 (1), 41–51. doi:10.1002/jobm.201700289
30. Jameel, M. S., Aziz, A. A., and Dheyab, M. A. (2020). Green Synthesis: Proposed Mechanism and Factors Influencing the Synthesis of Platinum Nanoparticles %. *J. Green. Process. Synth.* 9 (1), 386–398. doi:10.1515/gps-2020-0041
31. Kagithoju, S., Godishala, V., and Nanna, R. S. (2015). Eco-friendly and green Synthesis of Silver Nanoparticles Using Leaf Extract of Strychnos Potatorum Linn.F. And Their Bactericidal Activities. *3 Biotech.* 5 (5), 709–714. doi:10.1007/ s13205-014-0272-3
32. Kampa, M., Alexaki, V.-I., Notas, G., Nifli, A.-P., Nistikaki, A., Hatzoglou, A., et al. (2004). Antiproliferative and Apoptotic Effects of Selective Phenolic Acids on T47D Human Breast Cancer Cells: Potential Mechanisms of Action. *Breast Cancer Res.* 6 (2), R63. doi:10.1186/bcr752
33. Kawata, K., Osawa, M., and Okabe, S. (2009). *In Vitro* toxicity of Silver Nanoparticles at Noncytotoxic Doses to HepG2 Human Hepatoma Cells. *Environ. Sci. Technol.* 43 (15), 6046–6051. doi:10.1021/es900754q

ISSN: 0975-3583, 0976-2833 VOL14, ISSUE 09, 2023

34. Kayange, N., Kamugisha, E., Mwizamholya, D. L., Jeremiah, S., and Mshana, S. E. (2010). Predictors of Positive Blood Culture and Deaths Among Neonates with Suspected Neonatal Sepsis in a Tertiary Hospital. *Mwanza-Tanzania* 10 (1), 39. doi:10.1186/1471-2431-10-39